RESEARCH ARTICLE

WILEY SYNAPSE

Carbonic anhydrase inhibitor acetazolamide shifts synaptic vesicle recycling to a fast mode at the mouse neuromuscular junction

Nicolas Ivan Bertone[1]* | Ayelén Ivana Groisman[1]* ![ORCID] | Graciela Lujan Mazzone[2] |
Raquel Cano[3] | Lucia Tabares[3] ![ORCID] | Osvaldo Daniel Uchitel[1] ![ORCID]

[1]Instituto de Fisiología, Biología Molecular y Neurociencias (IFIBYNE-UBA-CONICET) and Departamento de Fisiología, Biología Molecular y Celular, Facultad de Ciencias Exactas y Naturales, Universidad de Buenos Aires, Ciudad Universitaria, Buenos Aires C1428EHA, Argentina

[2]Laboratorios de Investigación aplicada en Neurociencias (LIAN)—Fundación para la Lucha contra las Enfermedades Neurológicas de la Infancia (FLENI), CONICET, Buenos Aires, Argentina

[3]Department of Medical Physiology and Biophysics, School of Medicine, University of Seville, Seville 41009, Spain

Correspondence
Osvaldo Daniel Uchitel, Instituto de Fisiología, Biología Molecular y Neurociencias (IFIBYNE-UBA-CONICET) and Departamento de Fisiología, Biología Molecular y Celular, Facultad de Ciencias Exactas y Naturales, Universidad de Buenos Aires, Ciudad Universitaria, Buenos Aires C1428EHA, Argentina.
Email: ouchitel@gmail.com

Abstract

Acetazolamide (AZ), a molecule frequently used to treat different neurological syndromes, is an inhibitor of the carbonic anhydrase (CA), an enzyme that regulates pH inside and outside cells. We combined fluorescent FM styryl dyes and electrophysiological techniques at *ex vivo* levator auris longus neuromuscular junctions (NMJs) from mice to investigate the modulation of synaptic transmission and vesicle recycling by AZ. Transmitter release was minimally affected by AZ, as evidenced by evoked and spontaneous end-plate potential measurements. However, optical evaluation with FM-styryl dyes of vesicle exocytosis elicited by 50 Hz stimuli showed a strong reduction in fluorescence loss in AZ treated NMJ, an effect that was abolished by bathing the NMJ in Hepes. The remaining dye was quenched by bromophenol, a small molecule capable of diffusing inside vesicles. Furthermore, in transgenic mice expressing Synaptophysin-pHluorin (SypHy), the fluorescence responses of motor nerve terminals to a 50 Hz train of stimuli was decrease to a 50% of controls in the presence of AZ. Immunohistochemistry experiments to evaluate the state of the Myosin light chain kinase (MLCK), an enzyme involved in vesicle recycling, demonstrated that MLCK phosphorylation was much stronger in the presence than AZ than in its absence in 50 Hz stimulated NMJs. We postulate that AZ, via cytosol acidification and activation of MLCK, shifts synaptic vesicle recycling to a fast (kiss-and-run) mode, which changes synaptic performance. These changes may contribute to the therapeutic action reported in many neurological syndromes like ataxia, epilepsy, and migraine.

KEYWORDS

bromophenol, endocytosis, endplate potentials, exocytosis, FM styryl dyes, myosin light chain kinase, synaptophysin-pHluorin, transmitter release

1 | INTRODUCTION

The adult vertebrate neuromuscular junction (NMJ) is an extremely dependable synapse. To ensure effective excitation of the postsynaptic muscle fiber, the presynaptic terminal must exocytose a large number of vesicles with each stimulus and must be able to resupply a comparable number of

---

Abbreviations: AZ, acetazolamide; BPB, bromophenol; LAL, levator auris longus; NMJ, neuromuscular junction; pMLC2, phospho-myosin light chain 2; SypHy, synaptophysin-pHluorin; TPA, 12-O-tetradecanoylphorbol-13-acetate.

*Nicolas Ivan Bertone and Ayelén Ivana Groisman contributed equally to this work and are listed in alphabetic order.

vesicles by subsequent endocytosis or by recruitment from the reserve pool. Thus, the regeneration of synaptic vesicles after exocytosis at nerve terminals is critical for the maintenance of neurotransmission across a wide range of stimulation frequencies.

In the 1970s, Heuser and Reese described that vesicle fusion is followed by full collapse of the vesicle membrane into the plasma membrane and the recovery of the synaptic vesicle occurs at a slow speed (Heuser, 1989b; Heuser and Reese, 1973). At the same time, Ceccarelli, Hurlbut, & Mauro (1972, 1973) proposed that vesicle fusion involves the opening of a small pore, termed the 'fusion pore' (Breckenridge and Almers, 1987), followed by its rapid closure without full dilation and collapse. This model, referred to as "kiss-and-run" (Fesce, Grohovaz, Valtorta, & Meldolesi, 1994; He and Wu, 2007) was based mainly on the electron microscopic observations of motor nerve terminals but further support was obtained with electrophysiological and fluorescent methods in other preparations (Alés et al., 1999; Alvarez de Toledo, Fernández-Chacón, & Fernández, 1993; Harata, Choi, Pyle, Aravanis, & Tsien, 2006; Zhang, Li, & Tsien, 2009).

At the NMJ, frequency-dependent changes in the spatial location of endocytosis were demonstrated by Gaffield et al. (2009) based on the observation that exocytosis and endocytosis sites colocalize at high (100 Hz) but not at a lower (40 Hz) frequency of stimulation. The regulation of endocytosis at different stimulation frequencies is not well known yet but in a series of papers by Polo-Parada, Bose, & Landmesser (2001), Polo-Parada, Bose, Plattner, & Landmesser (2004) Polo-Parada, Plattner, Bose, & Landmesser (2005) an intracellular signaling pathway involving myosin light chain kinase (MLCK) and myosin II was shown to be required for effective transmission at adult mouse NMJs at high (100 Hz and above) but not at low (10 Hz) stimulus frequencies (Maeno-Hikichi, Polo-Parada, Kastanenka, & Landmesser, 2011).

High frequency stimulation (HFS) results in internal nerve terminal pH changes according to studies performed at NMJs constitutively expressing pH-sensitive Yellow Fluorescent Protein (Zhang, Nguyen, Barrett, & David, 2010). Interestingly, Ca^{2+} influx elicited by action potential trains (12.5–100 Hz) evokes a biphasic response consisting in a brief acidification followed by a prolonged alkalinization that outlasts the stimulation train, revealing the possibility that key components of vesicular neurotransmitter release can be affected by cytosolic pH. For example, acidification inhibits endocytosis (Dejonghe et al., 2016; Heuser, 1989a; Lindgren, Emery, & Haydon, 1997; Sandvig, Olsnes, Petersen, & van Deurs, 1987) and alkalinization seems to facilitate endocytosis (Zhang et al., 2010). Physiologically, one of the main regulators of the cellular pH is the enzyme CA, which catalyzes the rapid and reversible conversion of CO_2 and water to HCO_3^- and H^+ (Maren, 1967). In fact, the initial acidification reported by Zhang et al. (2010) is greatly enhanced by Acetazolamide (AZ), an inhibitor of the CA enzyme.

To get more insight into the regulation of vesicle recycling we studied the effect of AZ on synaptic transmission with electrophysiology, FM styryl dye (Betz and Bewick, 1992; Hoopmann, Rizzoli, & Betz, 2012), pHlourin (Tabares et al., 2007), and immunohistochemical measurements. Our results indicate that pH changes at nerve terminals during sustained electrical stimulation regulates neurotransmission and suggest that acidification, via activation of the MLKC pathway, switches the mode of exo/endocytosis to a fast vesicle recycling mode.

2 | MATERIALS AND METHODS

2.1 | Animal protocols

Experiments were carried out on the left LAL muscle of male C57BL/6 J mice (https://www.jax.org/strain/000664). Animals were supplied by the animal house of the school of Exacts and Natural Sciences of the University of Buenos Aires. Animals were cared for in accordance with national guidelines for the human treatment of laboratory animals, similar to those of the US National Institutes of Health. Animals were anesthetized with an overdose of 2% tribromoethanol (0.15 mL/10 g body weight) injected into the peritoneal cavity and exsanguinated immediately. The muscle with its nerve supply was excised and dissected on a Sylgard-coated Petri dish containing physiological saline solution of the following composition (in mM): 137 NaCl, 5 KCl, 2 $CaCl_2$, 1 $MgSO_4$, 12 $NaHCO_3$, 1 $Na2HPO_4$ and 11 glucose; continuously bubbled with 95% O_2 ╱ 5% CO_2; pH 7.4. The preparation was then transferred to a 1.5 mL recording chamber. Experiments were performed at room temperature (20–23°C).

2.2 | Electrophysiological recordings

Evoked (EPP) and spontaneous (MEPP) endplate potentials were recorded with conventional intracellular microelectrodes filled with 3 M KCl (5-15 MΩ). Electrophysiological experiments were performed in bicarbonate buffer. The nerve was stimulated via two platinum electrodes isolated with grease coupled to a pulse generator (Grass S88, Grass Inst., USA). To avoid muscle contraction, μ-conotoxin GIIIB (1 μM) was used. Intracellular recordings were obtained using an Axoclamp-2A amplifier in combination with a Digidata 1400A interface and commanded with pClamp 8.2 software (Axon Instruments, Molecular Devices, CA).

In each muscle fiber where quantal output was estimated, MEPPs were recorded during 100 s followed by a low frequency (0.33 Hz) stimulation during 36 s. AZ treated muscles were incubated in a 100 μM AZ solution for 30 min to 1 h before studied. Quantal content (QC) was determined by a direct method and corrected for nonlinear summation (McLachlan and Martin, 1981), using the formula below and MEPPs mean value from the last 20 s of 100 s recording.

$$QC = E/(m * (1 - 0.8E/V_m))$$

where E is the amplitude of an individual EPP, m is the mean amplitude of MEPPs, and V_m is the membrane potential. Amplitudes for both EPP and MEPPs were normalized to $V_m = -70$ mV, assuming 0 mV as the reversal potential for acetylcholine (ACh) nicotinic receptors.

2.2.1 | High frequency and bursts stimulation protocol

High frequency (50 Hz) nerve stimulation was applied up to a total of 7,300 pulses. Normalized EPP amplitudes and EPPs summed amplitudes were plotted for control and AZ-treated muscles.

During the ˙bursts˙ protocol, the nerve was stimulated with trains at high frequency (50 Hz) for 1 s followed by 1 s of rest. This sequence was repeated for a period of 1 min for control and AZ treated muscles. Normalized amplitude of the first and last EPP was analyzed for the 1st, 5th, 10th, 15th, 20th, and 30th train.

Absolute depression was quantified as the difference in amplitude between the first EPP of the first train and the last EPP of each short tetanic train. Relative depression was quantified as the difference in amplitude between the first and the last EPP inside each short tetanic train (1st, 5th, 10th, 15th, 20th, and 30th short tetanic trains were analyzed). For statistical calculations, student's t test for differences analysis, and f test for variance, in SigmaPlot 10.0 and Origin Pro 8 software were used.

2.3 | FM 2–10 imaging

FM 2–10 imaging experiments were performed in bicarbonate buffer and Hepes buffer (10 mM). To avoid muscle contraction, α-bungarotoxin (5 μM) was applied to the bath. All images were acquired with a high performance camera (Quantix camera, Photometrics, Tucson, AZ) and an optical filter changer Lambda 10–2 (Sutter Instrument, Novato, CA). Long loading protocol was used to fully load vesicle recycling pool (Perissinotti and Uchitel, 2010). Nerve terminals were incubated for 5 min with FM2–10 prior to the loading by 20 Hz nerve stimulation during 10 min. After 20-min washing, images were acquired to quantify the maximal loading. During a resting period of 30 min to 1 h, the muscles were treated or not with AZ (100 μM) and thereafter, the vesicle unloading protocol was performed at the selected stimulation frequency. Fluorescence images were acquired every 3 s during unloading.

2.3.1 | Bromophenol blue assay

After FM loading protocol and AZ treatment, bromophenol blue (2 mM) was incubated for 5 min and kept during the following unloading protocol as described before.

2.3.2 | Analysis of FM fluorescence signals

Fluorescence was quantified as the percentage of the maximum signal after load. Absolute fluorescence was converted to percentage of fluorescence with the following equation:

$$\%F(t) = (F(t) - F_{nv}/(F_{max} - F_{nv})) \times 100$$

Where $F(t)$ is the absolute fluorescence at time t, F_{max} the absolute fluorescence after maximum loading and F_{nv} is the nonvesicular fluorescence background (fluorescence remaining after treatment with 90 mM K+ for 5 min.)

Images were analyzed with Image J 1.49 software.

2.4 | Live imaging acquisition and analysis

Transgenic mice expressing SypHy as a fusion protein, under the neuron-specific promoter Thy 1.2 were used. This tool allowed us to study synaptic vesicle recycling in motor nerve terminals from the LAL muscle in real time by monitoring the fluorescence changes taking place during exocytosis and endocytosis. To monitor fluorescence changes, a Yokogawa CSU-X1 spinning disk system (3i, Göttingen, Germany) mounted on an upright BX61WI microscope (Olympus, Spain) was used. For excitation, a 488 nm laser was used. Images were acquired by means of a back-thinned EM-CCD camera C9100-13 (Hamamatsu, Spain) with an effective number of pixels of 512(H) × 512(V), and a pixel size of 16 × 16 μm^2. Images were acquired at 1 frames s^{-1} with commercial software (SlideBookTM 5.0, 3i). Before analysis, images were aligned, and regions of interest (ROIs) selected. After background subtraction, fluorescence changes (ΔF) were normalized with respect to the basal level (F_0). In all experiments, the nerve was stimulated twice at 50 Hz, during 75 s, first in the control solution, and after 30-min incubation in 100 μM AZ (final DMSO concentration: 0.1%). Recordings with only DMSO were not significantly different to controls. All experiments reported include the results of at least three animals per genotype. All experiments were performed according to the guidelines of the European Council Directive for the Care of Laboratory Animals.

2.5 | LAL phospho-myosin light chain 2 immunostaining

LAL muscles were dissected, as previously described, and incubated in saline with or without AZ (100 μM) for 30 min. Nerve was stimulated at 50 Hz for 10 min, and 30 s before the end of stimulation muscles were fixed in 4% paraformaldehyde in PBS (pH 7.4) for 10 min at 4°C, containing β-glycerophosphate (5 mM) and potassium fluoride (5 mM) to prevent dephosphorylation, and stored in 30% sucrose-PBS for cryoprotection (24 h at 4°C). LAL were permeabilized and blocked with 10% fetal calf serum (FCS), 2% bovine serum albumin (BSA), 0.5% Triton in PBS (blocking solution) for 1 h at room temperature. Muscles were incubated overnight at 4°C with an antibody against phospho-myosin light chain 2 (Ser19, anti-pMLC2 polyclonal,

Cell Signaling Technology, Danvers, MA; 1:50 dilution in 1% NGS, 1% BSA, and 0.1% Triton X-100 in PBS). After washing with PBS, the primary antibody was visualized with a subsequent 2 h incubation using a secondary antibody (anti-mouse Alexa Fluor 647, Invitrogen, Carlsbad, CA; 1:1,000 dilution in PBS) and postsynaptic nicotinic acetylcholine receptors with fluorochrome-conjugated α-bungarotoxin-FITC (Invitrogen Argentina S.A., Buenos Aires, Argentina; 1:500) at room temperature. The 12-O-tetradecanoylphorbol-13-acetate (TPA, 20 μM, gently provided by Prof. Eduardo Cánepa) was added to the bath for 1 h, to significant increased the pMLC fluorescence intensity, as previously described (Maeno-Hikichi et al., 2011).

After immunostaining, images were acquired with an FV300 confocal fluorescence microscope (Olympus Optical, Tokyo, Japan) equipped with an image-acquisition system and Fluoview 3.3 software (Olympus Optical). For each endplate, pMLC mean fluorescence intensity was obtained by densitometry analysis using stacks of 20–35 images (60$\times$ magnification, 1-μm interval) with a confocal microscope, always maintaining the same pinhole (airy 2) and the same confocal settings for comparison purpose between different samples. The resulting images were analyzed by using Image J software 1.42 software (National Institutes of Health, Bethesda, MD, http://imagejdocu.tudor.lu). Background fluorescence intensity, adjacent to the endplate, was subtracted to correct the pMLC mean endplate fluorescence intensity.

2.6 | Statistics

Results were expressed as means normalized fluorescence intensity$\pm$ SEM; n refers to the number of endplates, obtained from three different experiments. For statistical calculations, we used SigmaStat 3.11 (Systat Software, Chicago, IL). For multiple comparisons values were analyzed with the Kruskal-Wallis test, followed by the Tukey-Kramer post hoc test. Two groups of data were considered statistically different if $p \leq 0.05$.

2.7 | Toxin and chemicals

Acetazolamide (SIGMA) was dissolved in dimethyl sulfoxide (DMSO) at 100 mM. Tribromoethanol, α-bungarotoxin and all salts of analytical grade were purchased from Sigma (St. Louis, MO), and μ-conotoxin GIIIB was purchased from Alomone Labs (Jerusalem, Israel). Sucrose was purchased from Merck (Darmstadt, Germany).

3 | RESULTS

3.1 | Spontaneous and evoked transmitter release in AZ-treated NMJs

To gain insight on the role of CA on transmitter release we studied the effect of its inhibition by AZ on spontaneous and evoked release of acetylcholine at the mouse NMJ. Muscle fiber intracellular recordings of synaptic activity revealed that AZ had no effect on MEPP amplitude (0.72 ± 0.04 mV in AZ treated vs. 0.71 ± 0.04 mV in control), but AZ treated muscles showed an increase in MEPPs frequency (3.5 ± 0.3 MEPPs s^{-1} in AZ treated vs. 2.4 ± 0.2 MEPPs s^{-1} in control) ($n = 69$ fibers/8 AZ treated muscles and $n = 40$ fibers/7 control muscles) (**$p = 0.0006$), (Figure 1a,b).

Evoked nerve endplate potentials (EPPs) were recorded every 2 s in 2 mM Ca^{2+}/1 mM Mg^{2+}, in the presence of μ-conotoxin GIIIB (1 μM) to avoid muscle contraction. Quantal content was estimated using the amplitude of the MEPPs previously measured in the same muscle fiber (direct method, corrected for nonlinear summation, see Materials and methods). A small but significant decrease in quantal content was observed. Mean quantal content in AZ-treated muscles was 24.4 ± 1.3 ($n = 59/7$) and in control was 30.4 ± 1.5 ($n = 34/6$), (*$p = 0.007$) (Figure 1c).

To further assess the effect of carbonic anhydrase on exocytosis and vesicle replenishment, transmitter release at HFS was studied in AZ-treated NMJs. During 50 Hz stimulation trains EPP amplitudes underwent short-term depression (Figure 1d,f). The time course and the final level of depression were not affected by AZ treatment. (y0 control 0.25 ± 0.02 mV and AZ 0.19 ± 0.03 mV; tau control 31 ± 5 s and 31 ± 5 s tau AZ; n: control $= 19/5$ and AZ $= 12/4$). Furthermore, the summed normalized amplitudes during HFS trains showed no significant differences between control and AZ treated muscles (Figure 1e; $n = 19/5$ in control and 12/4 in AZ).

To further analyze the effect of AZ on vesicle replenishment, short bursts of HFS were applied repetitively during 60 s (50 Hz, 1 s, every 2 s). The relative depression after 30 bursts was of $23\% \pm 3\%$ in control vs. $21\% \pm 3\%$ in AZ treated muscle. Furthermore, the depression at the end of the 30st burst was also similar ($52\% \pm 5\%$ control vs. $42\% \pm 7\%$ AZ treated). In summary, no differences were observed between control and AZ treated muscles (Figure 1g).

These results suggested that CA inhibition has no effect on ACh release and ACh replenishment except for a small reduction of quantal content value in agreement with previously reported data by Kaja, Frants, Ferrari, Van Den Maagdenberg, & Plomp (2008).

3.2 | Differential effect of AZ at different stimulation frequencies

To have a different approach on the influence of carbonic anhydrase activity on the dynamics of exo- and endocytosis we examined the time course of FM 2–10 destaining at motor nerve terminals in the presence or not of AZ (Figure 2a). Nerve terminals were maximally loaded with FM2–10 (10 min at 20 Hz, see Materials and methods), and then destained at different frequencies.
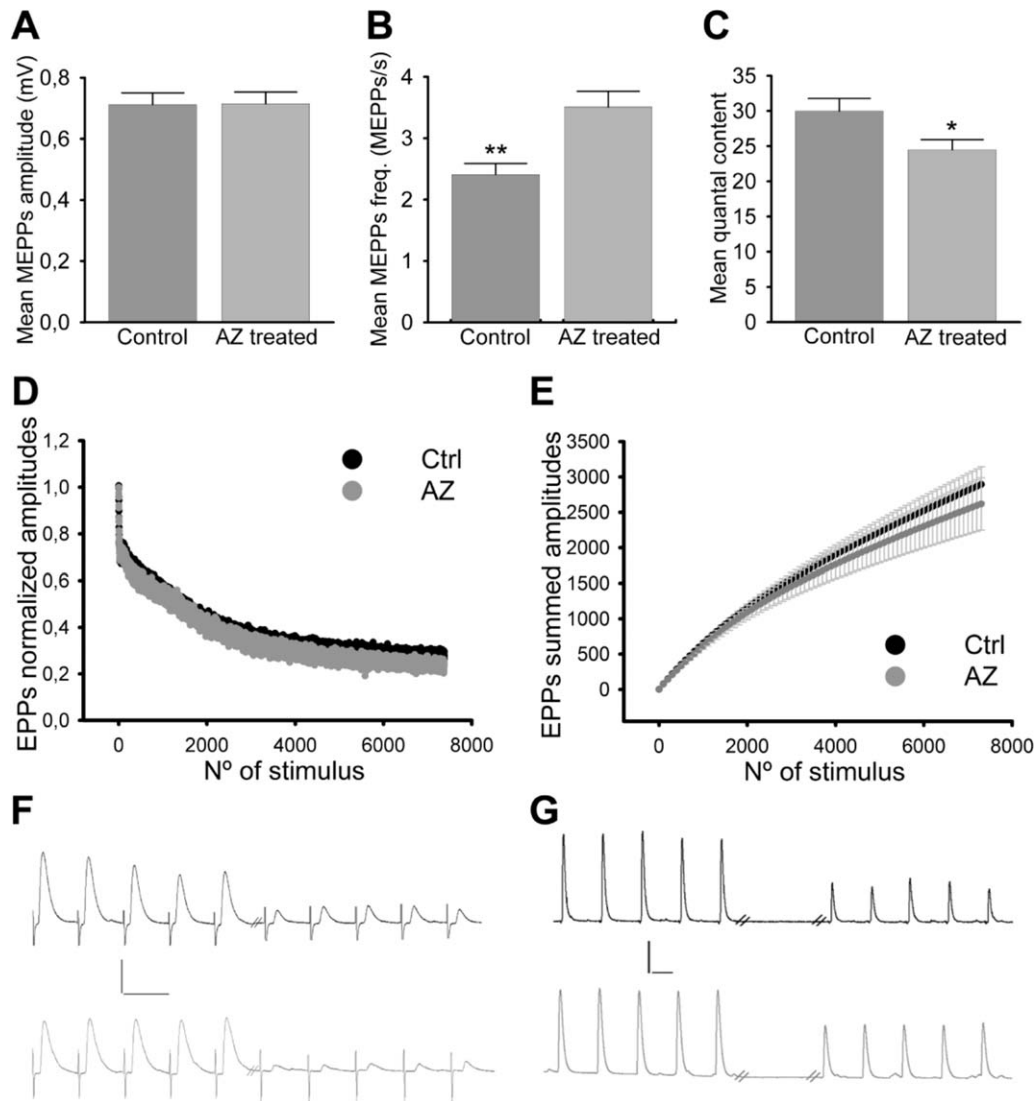
FIGURE 1 Effect of AZ on spontaneous and evoked neurotransmitter release. Mean MEPP amplitudes in control and AZ treated muscles were similar (a) while augmented MEPP mean frequency was observed in AZ treated muscles (b). AZ reduces the mean quantal content at low stimulation frequency (0.33 Hz) (c). However, no differences were observed when transmitter release was evoked at high frequency (50 Hz). EPPs normalized amplitudes vs number of stimuli shows similar depression for control and AZ treated muscles when stimulated at 50 Hz (d). Summed EPP amplitudes during high frequency stimulation trains showed no significant differences between control (n =12/4) and AZ-treated (n = 19/5) terminals (e). (f) Representative EPP traces at 50 Hz frequency stimulation. Note the huge amplitude reduction after long lasting stimulation of control (black trace) and AZ-treated (gray trace) muscles. Scale bars: 1 mV, 10 ms (g) Representative traces of EPPs when bursts stimulation was performed. Absolute and relative depressions were not different. Scale bars: 10 mV, 10 ms

Figure 2b shows the time course of nerve terminal destaining at 10, 50, and 100 Hz. In control experiments, at 10 and 50 Hz, fluorescence loss was rapid with approximately 50% of the dye being released by the 5000th stimulus (Figure 2b). However, with 100 Hz, only 34% of the fluorescence was lost by the same amount of stimulus. In the presence of AZ, no effect on the kinetics of FM fluorescence loss was seen at 10 Hz stimulation, but at 50 Hz only 19% of destaining by the 5,000th stimulus was observed. At 100 Hz stimulation, fluorescence loss was already slow in control and AZ-treated terminals (Figure 2c). We next compared vesicle exocytosis estimated by quantal content and by FM destaining (Figure 2e) at the same stimulation frequency and confirmed the discrepancy between these two measurements.

To investigate if the slowing effect of AZ on FM fluorescence loss upon stimulation was due to pH changes we compare the extend, and rate, of destaining in control and AZ-treated muscles incubated in bicarbonate or in Hepes buffer solution and stimulated at 50 Hz. Figure 2d shows that the slowing effect of AZ on FM destaining is completely suppressed by the presence of the strong buffer capacity of Hepes. After prolonged stimulation, fluorescence loss in AZ-treated muscles in Hepes buffer was 67% ± 2%, with an exponential decay tau of 53 ± 13 s (n = 5) similar to non-treated control muscles (74% ± 4%, tau: 59 ± 7 s, n = 8, p = 0.35). In contrast, fluorescence loss and tau were much reduced, (32% ± 6%, tau: 24 ± 2 s, n = 7) in AZ-treated compare to nontreated in control bicarbonate buffer (76% ± 4%, tau: 52 ± 13, n = 7, p = 0.007). In summary, in the
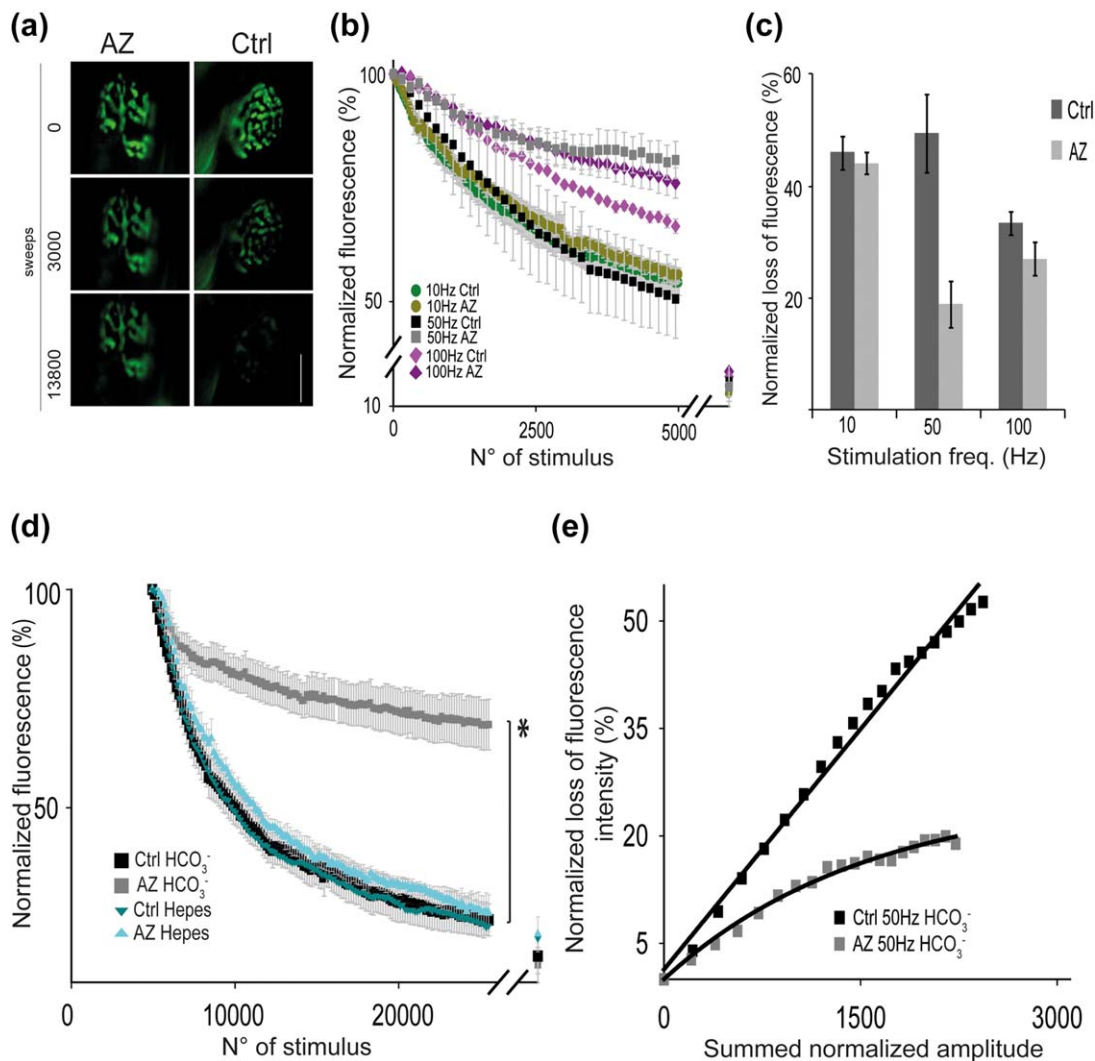
FIGURE 2 FM destaining at 50 Hz is strongly reduced by AZ in bicarbonate but not in Hepes buffer. (a) Examples of fluorescent endplates images, stained with FM 2–10 at the beginning, middle and end of the high frequency stimulation protocol (50Hz). (Scale bar, 10 μM). (b, c) Destaining under different frequency stimulation protocols in bicarbonate buffer, showing destaining kinetics and normalized fluorescence loss (FL) for control and AZ treated muscles. FL after 5,000 stimuli (c) at low frequency stimulation protocol (10 Hz) was 46% ± 3%, tau = 66 ± 13 s, $n = 5$ for control and 44% ± 2%, tau: 50 ± 12 s, $n = 5$ for AZ-treated muscles. At 50 Hz stimulation protocol, FL was 49% ± 9%, tau: 76 ± 4 s, $n = 7$ and 19% ± 4%, tau: 24 ± 2 s., $n = 7$ for control and AZ-treated muscles respectively. At 100 Hz stimulation protocol, FL was 34% ± 2% $n = 6$, tau: 26 ± 2 s for control and 27% ± 3%, tau: 24 ± 2 s $n = 6$, for AZ-treated muscles. Data from three to four muscles. (d) The 50-Hz stimulation protocol was performed in bicarbonate and in stronger buffer capacity (Hepes 10 mM) for 20,000 stimuli to study long lasting unloading dynamics in control and AZ-treated muscles. In Hepes buffer, destaining in AZ treated muscles was 67% ± 2%, tau: 53 ± 13 s, $n = 5$, and for control was 74% ± 4%, tau: 59 ± 7 s, $n = 8$, ($p = 0.3481$), while in bicarbonate buffer AZ-treated muscles destaining was 32% ± 6%, tau: 24 ± 2 s $n = 7$ and for control 76% ± 4%, tau:52 ± 13 s $n = 7$ ($p = 0.0071$). Data obtained from three to four muscles. (e) Normalized loss of fluorescence intensity vs summed normalized amplitude at 50 Hz stimulation shows the linear correlation between the imaging and electrophysiological experiments for control muscles $f = y0 + a \times x$ where $y0 = 1.4$ and $a = 0.02$ while for AZ-treated muscles the adjustment was exponential. $F = a \times (1 - \exp(-b \times x))$ where $a = 26$ and $b = 6 \times 10^{-4}$

experiments performed in Hepes buffer (control and AZ NMJs) versus bicarbonate AZ treated NMJs, the fluorescence loss was significantly different ($p = 0.0095$ and 0.026, respectively). Data obtained from three muscles in Hepes and four muscles in bicarbonate buffer.

3.3 | Bromophenol (BPB) is able to quench dye retained in synaptic vesicle

We have shown that in the presence of AZ, NMJs stimulated at 50 Hz continue to release ACh but much less FM dye was released than predicted by the summed quantal content (Figure 2e). The retained dye could result from the reuse of a fraction of vesicles already destained during previous fusion or from fast exo-/endocytosis cycles preventing dye unloading, but allowing ACh release.
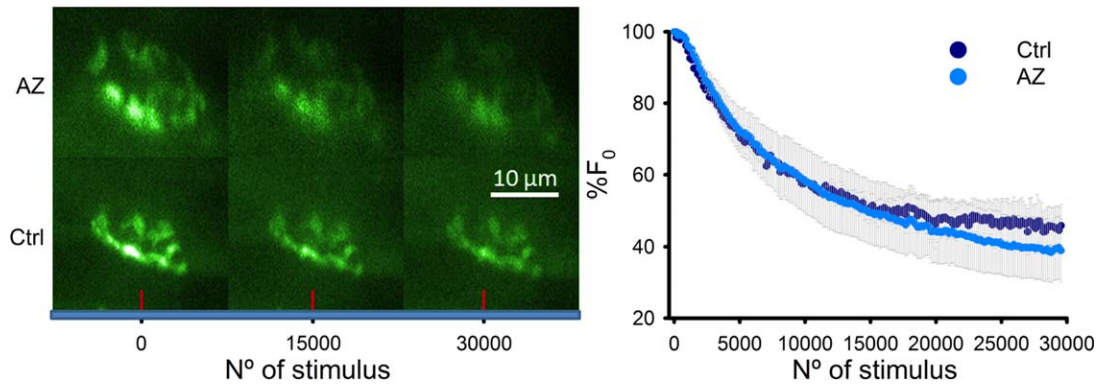
FIGURE 3 Retained FM dye-quenched by Bromophenol reveal that most dye-loaded vesicles are exocytosed at 50 Hz in the presence of AZ. Bromophenol Blue (2 mM) was applied at control and AZ-treated muscles in bicarbonate buffer and a 50-Hz unloading protocol was applied. AZ-treated muscles showed a fraction of fluorescence loss of similar to the fraction of fluorescence loss at control muscles ($62.1\% \pm 8.8\%$, tau $= 41 \pm 13$ s, $n = 5$ vs. 56, $7\% \pm 6.3\%$, tau $= 42 \pm 9$ s, $n = 3$. t test $p > 0.05$). Data obtained from 3 muscles in control and 5 muscles in AZ

To further test whether FM dye is retained in synaptic vesicles after exocytosis we used BPB a small negatively charged molecule capable of quenching the fluorescent dye inside the vesicles even during rapid endocytosis or/and in the absence of full vesicle fusion (Harata et al., 2006). Therefore, in the presence of BPB all the vesicles that undergo exocytosis will be quenched. This should give us some insight whether a fraction of vesicles are rapidly reused or most of the vesicles undergo a fast endo-/exocitotic recycling.

After synaptic vesicles were fully loaded with FM dye and the dye was removed from the bath, BPB was applied to reach a 1 mM concentration. To overcome the light filtering effect produced by the presence of BPB solution between the nerve terminal and the objective we used a 40x short distance objective. Although the overall signal was reduced, it was enough to record the time course and extend of fluorescence loss during a 50 Hz stimulation train. As shown in Figure 3, AZ-treated and control muscles show no differences in fluorescence loss in the presence of 1 mM BPB-bicarbonate buffer condition (AZ: $62.1\% \pm 8.8\%$ loss, decay tau $= 41 \pm 13$ s, ($n = 5$); control: $56.7\% \pm 6.3\%$ loss, decay tau $= 42 \pm 9$ s ($n = 3$)). Thus the similar decrease in fluorescence in the presence or absence of AZ suggest that a fraction of vesicles undergo fast endocytosis.

3.4 | AZ reduces SypHy signal upon HFS

To further explore the role of CA on transmitter release we studied the effect of AZ on exocytosis and vesicle recycling in transgenic mice expressing SypHy. This fluorophore is tethered inside synaptic vesicles, where its fluorescence is acid-quenched. Upon exocytosis, SypHy is dequenched, and the fluorescence signal rises. Endocytosis and reacidification reverse the process (Tabares et al., 2007; Cano, Ruiz, Shen, Tabares, & Betz, 2012). During repetitive stimulation, the peak amplitude of the fluorescence change depends not only on the amount of pHluorin incorporated in the plasma membrane during exocytosis but also on that retrieved by endocytosis (Sankaranarayanan & Ryan, 2001).

We first compared the fluorescence responses of nerve terminals in the absence and the presence of 100 μM AZ in preparations bathed with the standard extracellular solution containing bicarbonate and gassed with 5% CO_2/95% O_2. The basal fluorescence at the nerve terminal was not significantly different in the absence or the presence of the drug (1721 ± 309 vs. 1401 ± 384 a.u, respectively; $n = 6$). We found that after 30-min incubation with AZ the peak amplitude of the fluorescent signal decreased in comparison with the response to the first train of stimulation in the absence of AZ (Figure 4a, $n = 6$), but did not affect the recovery of fluorescence after the stimulus train (Figure 4b). In the absence of AZ, the fluorescence peak amplitude during the second train was not significantly different to that of the first train ($n = 3$; $p = 0.77$); however, in the presence of the drug the peak decreased about 50% ($n = 6$; $p = 0.0008$) (Figure 4c). The fluorescence decay time constants of the second train normalized to the first train did not significantly change neither in presence nor absence of the drug (Figure 4d). The fluorescence change versus time of the first and second responses in control conditions (upper panel) and in the presence/absence of AZ (lower panel) are shown in Figure 4e.

To investigate if the effect of AZ on the amplitude of the fluorescent response was pH-dependent, we performed the same experiments in Hepes buffer extracellular solution. Figure 4f–h shows that neither the peak amplitude of the fluorescent responses during the trains or the decay kinetics after the stimuli were affected by the presence of AZ in the solution ($n = 3$).

3.5 | AZ enhances MLCK phosphorylation

In agreement with previous reports, our data suggest that HFS at the adult mouse NMJ switches the mechanism of vesicle cycling to a rapid-reuse mode (Maeno-Hikichi et al., 2011). MLCK is known to regulate vesicle trafficking and synaptic transmission, and activation of MLCK accelerates both slow and rapid forms of vesicle endocytosis at the calyx nerve terminals (Yue and Xu, 2014). MLCK signaling pathway is required to maintain
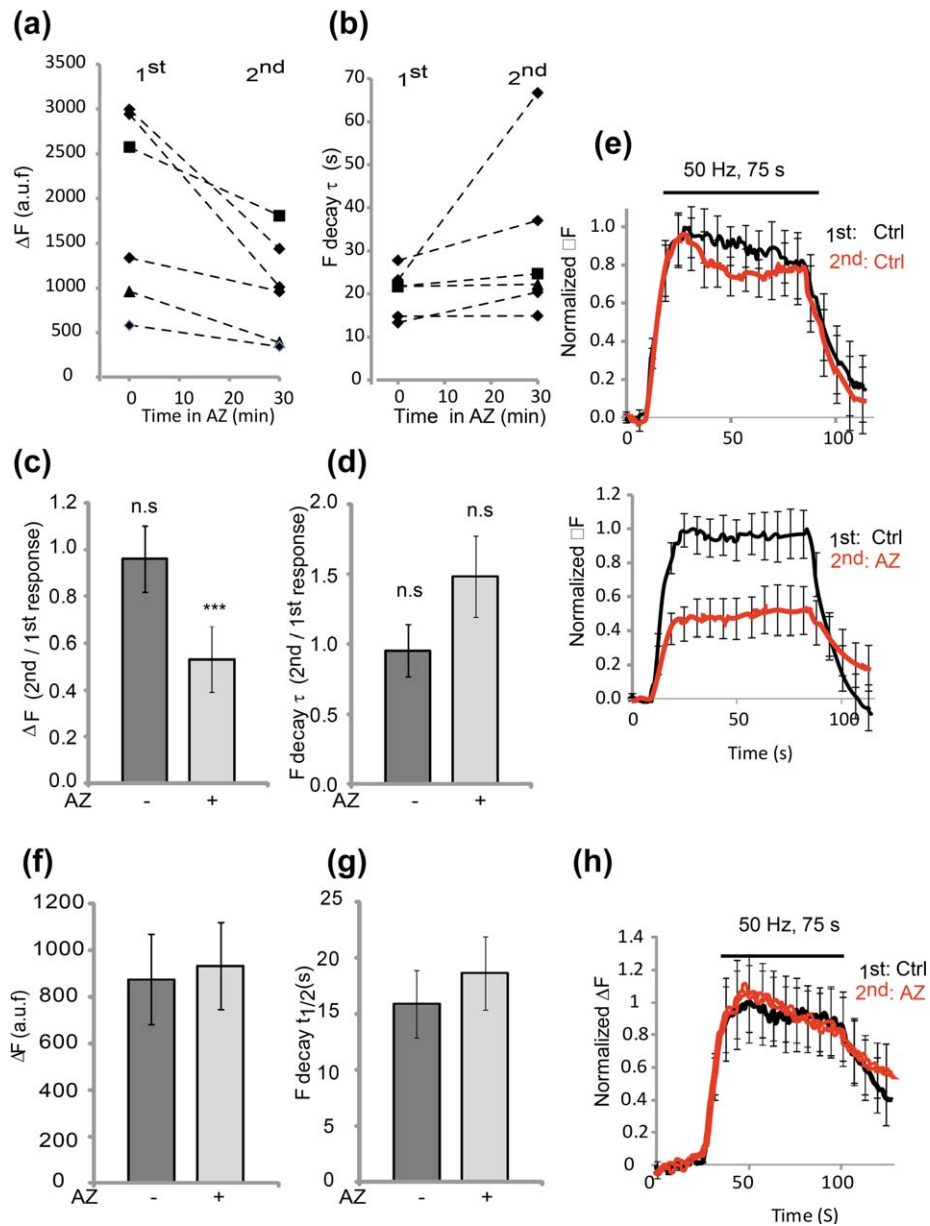
FIGURE 4 AZ decreases the amplitude of the fluorescent response in SypHy motor nerve terminals. (a) Change in peak fluorescence amplitude in response to two stimulation trains (50 Hz, 75 s) in the absence (1st train, $t = 0$) and in the presence of 100 μM AZ (2nd train, $t = 30$ min). Note that AZ reduced the amplitude of the responses in all cases ($n = 6$, six muscles). (b) Fluorescence decay time constants after stimulation in the absence and in the presence of the drug, same terminals as in (a). (c) In the absence of the drug, the mean peak response to the second train, normalized to the first train amplitude, did not change (dark bar); ($n = 3$). In the presence of AZ (light bar), the mean response was significantly reduced during the second train ($n = 6$). (d) The normalized mean time constants of the fluorescence decay were not different in the absence (dark bar) or in the presence of the drug AZ (light bar). (e) Upper graph: first (black trace) and second (red trace) mean responses to the two stimulation trains in the absence of the drug. Lower graph: mean fluorescence change in response to the first train in the absence (black) and after 30-min incubation with AZ (red). (f-h) same as before but using Hepes instead of bicarbonate/CO_2buffer ($n = 3$).Error bars are s.e.m. ***$p = 0.0008$

effective transmission at high stimulation frequencies (Polo-Parada et al., 2001, 2004). Furthermore, it has also been reported that AZ induces phosphorylation of myosin kinase facilitating the translocation of membrane proteins onto cell membrane (Zhang et al., 2012). To investigate the possible involvement of the MLCK in the mechanism of action of AZ we studied the state of phosphorylation of the enzyme in control and AZ treated muscles, with and without electrical stimulation (50 Hz).

We performed immunohistochemistry using an antibody against phospho-myosin light chain 2 (pMLC2). This antibody was previously used to demonstrate the involvement of MLCK activation at HFS (Maeno-Hikichi et al., 2011). Muscles were kept in control saline with or without AZ for at least 30 min before 50 Hz stimulation was applied for 10 min. Before the end of stimulation (30 s), muscles were fixed with paraformaldehyde and
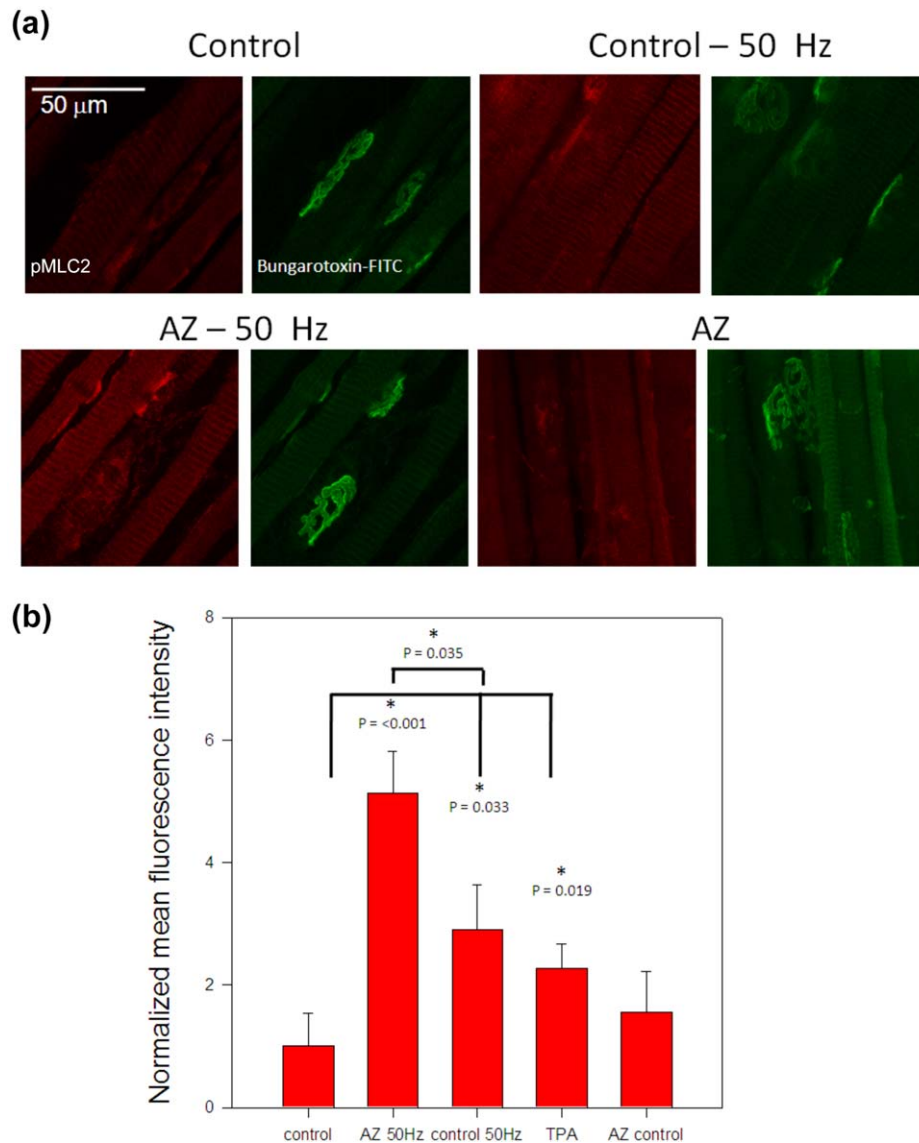
FIGURE 5 pMLC2 is upregulated with 50-Hz stimulus and AZ treatment. (a) Examples of confocal endplate images, staining in green with α-bungarotoxin-FITC, showing pMLC2 positive staining (red). Note that pMLC2 labeling was much larger in stimulated endplates at 50 Hz, and the staining was significantly increased when AZ (100 μM) was applied. pMLC2 staining was significantly increased with TPA (20 μM). (b) Histogram showing pMLC2 positive endplates as normalized mean fluorescence intensity from control; $n = 41–22$ from three different muscles

processed for immunohistochemistry evaluation (see Methods). Figure 5 shows confocal endplates images where the pMLC2 positive staining co-localized with the postsynaptic marker α-bungarotoxin-FITC. The degree of pMLC2 labeling was much larger in stimulated endplates at 50 Hz, and the staining was significantly increased when AZ was applied. As a control, the fluorescent signals of pMLC2 in muscles treated with TPA (20 μM) were measured and found to be significantly increased.

4 | DISCUSSION

In this work we confirm that at the adult mouse NMJ, AZ generates a small reduction on transmitter release quantal output at low stimulation frequency, in agreement with a previous report (Kaja et al., 2008). However, by combining electrophysiological data and optical evaluation of vesicle exocytosis at different frequencies we observed that AZ treatment results in dissociation between quantal output and vesicle destaining.

One of the characteristics of exo-/endocytosis during HFS is that allows the complete release of acetylcholine but partially impedes the exchange of molecules partitioned with the membrane like FM styryl dyes (Stevens and Williams, 2000; Pyle, Kavalali, Piedras-Rentería, & Tsien, 2000). We have shown that the amount of FM fluorescence loss differs at different stimulation frequencies even for the same number of vesicles

undergoing exocytosis. At 10 and 50 Hz, stimulation fluorescence loss was rapid, however, at 100 Hz, much less dye was lost. This lower amount of destaining suggests that the actual release mechanism may have changed with high frequency stimulation. As postulated by Maeno-Hikichi et al. (2011) differences in destaining rate between different stimulation regimes is not due to a different degree of depression but to a distinct form of exo-endocytosis that loses less FM dye. On top of this frequency modulation, treatment with AZ strongly reduces fluorescence loss at 50 Hz stimulation with no effect on FM fluorescence loss at 10 Hz indicating that AZ shifts the threshold to change the release mode to lower frequency values suggesting a synergic effect of HFS and CA inhibition. Furthermore, at motor nerve terminals of transgenic mice expressing SypHy the fluorescence responses to a 50 Hz train in the presence of AZ was decrease to a 50%. It is unlike that the decrease in peak amplitude of the fluorescent signal could be due to a reduction in exocytosis since AZ treatment results in a negligible reduction in quantal content. Alternative explanations are rapid endocytosis and reacidification resulting from a more acid cytosolic environment, or an increase in rapid local vesicle recycling. An indication that AZ affects release mode resulting in retention of FM dye in synaptic vesicles after exocytosis is provided by BPB quenching effect. Because of its small size and charge BPB easily enters and quench any remaining intravesicular fluorescence suggesting that AZ together with HFS favor a "kiss-and-run" mode of vesicle exocytosis instead a fast local reuse recycling mode which will quench only a limited number of vesicles.

Inhibitors of the CA enzyme like AZ are used to treat ataxias, dizziness and other neurological syndromes (Bagnato and Good, 2016; Kotagal, 2012; Ogawa, 2004). CA is present in many tissues of the body, including the brain, where catalyzes a reversible reaction between CO_2 hydration and HCO_3^- dehydration. However, the mechanisms of how this therapeutic effect is achieved are not known (Bueno-Junior et al., 2017; Ruusuvuori and Kaila, 2014).

Zhang et al. (2010) used the pH-sensitive fluorescence of Yellow Fluorescent Protein transgenically expressed in mouse motor nerve terminals to report pH changes due to presynaptic stimulation. Ca^{2+} influx elicited by action potential trains evokes a biphasic intracellular pH change composed by a brief initial acidification followed by a prolonged alkalinization which outlasts the stimulation train. The initial acidification results from the extrusion of the elevated cytosolic $[Ca^{2+}]$ by activation of the plasma membrane Ca^{2+}-ATPase (PMCA), which admits H^+ to the nerve terminal and extrudes Ca^{2+} to the extracellular space. At this stage, H^+ entry via the PMCA exceeds H^+ extrusion via other transporters and particularly the vesicular H^+-ATPase (vATPase). The incorporation of vATPase in the presynaptic membrane due to the collapse of synaptic vesicles results in a strong efflux of H^+. This later alkalinization seems to facilitate clathrin-dependent endocytosis. On the other hand, the initial cytosolic acidification could reduce the sensitivity of internalization of clathrin-coated pits from the plasma membrane and of dynamin-adaptin binding (Davoust, Gruenberg, & Howell, 1987; Heuser, 1989a; Sandvig et al., 1987; Wang, Südhof, & Anderson, 1995) reducing clathrin-dependent endocytosis. Interestingly, AZ as shown by Zhang et al. (2010) increases the initial acidification without much effect on the alkalinization. Therefore, it is possible that acidification will promote a clathrin-independent endocytosis mode, in agreement with the effect of AZ on FM destaining. Further indications that AZ mechanism of action involves intracellular pH changes derive from experiments where the dissociation observed between transmitter release and FM destaining in AZ treated NMJs was abolished in the presence of a Hepes high buffer capacity bath solution. Similarly, high buffer capacity abolishes the reduction in the SypHy fluorescence responses to a 50 Hz train in the presence of AZ observed in bicarbonate/CO_2 buffer.

It has been demonstrated that MLCK is an important activity-dependent regulator of synaptic strength in several synapses. MLCK plays a crucial role in determining the size of the pool of synaptic vesicles that undergo fast release at a central nervous system synapse (González-Forero et al., 2012; Srinivasan, Kim, & von Gersdorff, 2008). At the NMJ, MLCK activity following repetitive stimulation is required to convey and/or exocytose synaptic vesicles at sufficient rates to maintain effective transmission (Maeno-Hikichi et al., 2011; Polo-Parada et al., 2005). In many cellular functions, MLCK acts downstream of Ca^{2+}/calmodulin and activates the functions of myosin by phosphorylation of its regulatory light chain. Activity-dependent regulation of endocytosis is a multiple steps process that involves many different lipid and protein molecules (Saheki and De Camilli, 2012). Indeed, endocytosis is significantly accelerated in response to strong Ca^{2+} and, may be achieved through different pathways including a recently proposed calmodulin/MLCK/myosin pathway. Li, Wu, Yue, Zhu, & Xu (2016), have recently shown that MLCK at hippocampal boutons functions downstream of Ca^{2+}/calmodulin to facilitate endocytosis through phosphorylation of MLC. At the NMJ Maeno-Hikichi et al. (2011) have shown that MLCK–myosin II pathway was required for effective transmission at 100 Hz and that activation of MLCK, reduces the amount of FM dye lost suggesting that activation of the enzyme switches the mechanism of vesicle cycling to a rapid-reuse mode and is required to sustain effective transmission in adult mouse NMJ. In agreement with the reported role of MLCK, our immunohistochemistry experiments performed to evaluate the state of phosphorylation of the MLCK have shown that NMJ labeled with an antibody against phospho-myosin light chain was much larger in stimulated endplates at 50 Hz, and the staining was significantly increased when stimulation and AZ treatment were combined. Interestingly, there are some evidence that MLCK activity is altered by pH changes (Blumenthal & Stull, 1982) and also there are some indications of a possible direct activation of myosin kinases by AZ (Zhang et al., 2012) in human kidney cells. Thus, Ca^{2+} levels, acidification and direct effect on the enzyme could mediate AZ activation of MLCK, but the precise mechanisms need to be further investigated. Other factors like temperature, known to affect the rate of endocytosis and vesicle mobilization (Kushmerick, Renden, & von, 2006; Renden and von Gersdorff, 2007; Ruiz et al., 2011), that might also change the mode of vesicle recycling need further experimental validation.

In summary, the present study suggests that AZ via cytosol acidification and activation of MLCK accelerates vesicle endocytosis in synapses what can contribute to sustain neurotransmission during repetitive activity. This effect of AZ could modify synaptic performance in CNS synapses contributing to its therapeutic action reported in many neurological syndromes like ataxia, epilepsy and migraine.

ACKNOWLEDGMENTS

ORCID

Osvaldo Daniel Uchitel http://orcid.org/0000-0002-8909-6787
Ayelen Ivana Groisman http://orcid.org/0000-0003-2309-7055
Lucia Tabares http://orcid.org/0000-0002-4027-4044

REFERENCES

Alés, E., Tabares, L., Poyato, J. M., Valero, V., Lindau, M., & Alvarez de Toledo, G. (1999). High calcium concentrations shift the mode of exocytosis to the kiss-and-run mechanism. *Nature Cell Biology*, *1*(1), 40–44.

Alvarez de Toledo, G., Fernández-Chacón, R., & Fernández, J. M. (1993). Release of secretory products during transient vesicle fusion. *Nature*, *363*(6429), 554–558.

Bagnato, F., & Good, J. (2016). The use of antiepileptics in migraine prophylaxis. *Headache*, *56*(3), 603–615.

Betz, W. J., & Bewick, G. S. (1992). Optical analysis of synaptic vesicle recycling at the frog neuromuscular junction. *Science 10*, *255*(5041), 200–203.

Blumenthal, D. K., & Stull, J. T. (1982). Effects of pH, ionic strength, and temperature on activation by calmodulin a catalytic activity of myosin light chain kinase. *Biochemistry*, *21*(10), 2386–2391.

Breckenridge, L. J., & Almers, W. (1987). Currents through the fusion pore that forms during exocytosis of a secretory vesicle. *Nature*, *328*, 814–817.

Bueno-Junior, L. S., Ruggiero, R. N., Rossignoli, M. T., Del Bel, E. A., Leite, J. P., & Uchitel, O. D. (2017). Acetazolamide potentiates the afferent drive to prefrontal cortex in vivo. *Physiological Reports*, *5*(1), pii: e13066.

Cano, R., Ruiz, R., Shen, C., Tabares, L., & Betz, W. J. (2012). The functional landscape of a presynaptic nerve terminal. *Cell Calcium*, *52*(3/4), 321–326.

Ceccarelli, B., Hurlbut, W. P., & Mauro, A. (1972). Depletion of vesicles from frog neuromuscular junctions by prolonged tetanic stimulation. *The Journal of Cell Biology*, *54*, 30–38.

Ceccarelli, B., Hurlbut, W. P., & Mauro, A. (1973). Turnover of transmitter and synaptic vesicles at the frog neuromuscular junction. *The Journal of Cell Biology*, *57*, 499–524.

Davoust, J., Gruenberg, J., & Howell, K. E. (1987). Two threshold values of low pH block endocytosis at different stages. *The Embo Journal*, *6*, 3601–3609.

Dejonghe, W., Kuenen, S., Mylle, E., Vasileva, M., Keech, O., Viotti, C., ... Russinova, E. (2016). Mitochondrial uncouplers inhibit clathrin-mediated endocytosis largely through cytoplasmic acidification. *Nature Communications*, *7*, 11710.

Fesce, R., Grohovaz, F., Valtorta, F., & Meldolesi, J. (1994). Neurotransmitter release, fusion or 'kiss and run'? *Trends in Cell Biology*, *4*, 1–4.

Gaffield, M. A., Tabares, L., Betz, W. J. (2009). The spatial pattern of exocytosis and post-exocytic mobility of synaptopHluorin in mouse motor nerve terminals. *J Physiol*, *587*(6), 1187–200.

González-Forero, D., Montero, F., García-Morales, V., Domínguez, G., Gómez-Pérez, L., García-Verdugo, J. M., & Moreno-López, B. (2012). Endogenous Rho-kinase signaling maintains synaptic strength by stabilizing the size of the readily releasable pool of synaptic vesicles. *The Journal of Neuroscience : The Official Journal of the Society for Neuroscience*, *32*(1), 68–84.

Harata, N. C., Choi, S., Pyle, J. L., Aravanis, A. M., & Tsien, R. W. (2006). Frequency dependent kinetics and prevalence of kiss and run and reuse at hippocampal synapses studied with novel quenching methods. *Neuron*, *49*(2), 243–256.

Heuser, J. E. (1989a). Effects of cytoplasmic acidification on clathrin lattice morphology. *The Journal of Cell Biology*, *108*, 401–411.

Heuser, J. E. (1989b). Review of electron microscopic evidence favouring vesicle exocytosis as the structural basis for quantal release during synaptic transmission. *Quarterly Journal of Experimental Physiology*, *74*, 1051–1069.

He, L., Wu, L. G. (2007). The debate on the kiss-and-run fusion at synapses.*Trends Neurosci*, *30*(9), 447–455.

Heuser, J. E., & Reese, T. S. (1973). Evidence for recycling of synaptic vesicle membrane during transmitter release at the frog neuromuscular junction. *The Journal of Cell Biology*, *57*, 315–344.

Hogan, B., Constantini, F., & Lacey, E. (1994). Manipulating the mouse embryo: A laboratory manual. Cold Spring Harbor, NY: Cold Spring Harbor Laboratory.

Hoopmann, P., Rizzoli, S. O., & Betz, W. J. (2012). Imaging synaptic vesicle recycling by staining and destaining vesicles with FM dyes. *Cold Spring Harbor Protocols 1 2012*(1), 77–83.

Kaja, S., Frants, R. R., Ferrari, M. D., Van Den Maagdenberg, A. M., & Plomp, J. J. (2008). Reduced ACh release at neuromuscular synapses of heterozygous leaner Ca(v)2.1-mutant mice. *Synapse (New York, N.Y.)*, *62*(5), 337–344.

Kotagal, V. (2012). Acetazolamide-responsive ataxia. *Seminars in Neurology*, *32*(5), 533–537.

Kushmerick, C., Renden, R., & von, G. H. (2006). Physiological temperatures reduce the rate of vesicle pool depletion and short-term depression via an acceleration of vesicle recruitment. *Journal of Neuroscience*, *26*(5), 1366–1377.

Li, L., Wu, X., Yue, H. Y., Zhu, Y. C., & Xu, J. (2016). Myosin light chain kinase facilitates endocytosis of synaptic vesicles at hippocampal boutons. *Journal of Neurochemistry*, *138*(1), 60–73.

Lindgren, C. A., Emery, D. G., & Haydon, P. G. (1997). Intracellular acidification reversibly reduces endocytosis at the neuromuscular junction. *Journal of Neuroscience*, *17*, 3074–3084.

Maeno-Hikichi, Y., Polo-Parada, L., Kastanenka, K. V., & Landmesser, L. T. (2011). Frequency-dependent modes of synaptic vesicle endocytosis and exocytosis at adult mouse neuromuscular junctions. *The Journal of Neuroscience : The Official Journal of the Society for Neuroscience*, *31*(3), 1093–1105.

Maren, T. H. (1967). Carbonic anhydrase: Chemistry, physiology, and inhibition. *Physiological Reviews*, *47*(4), 595–781.

McLachlan, E. M., & Martin, A. R. (1981). Nonlinear summation of end-plate potentials in the frog and mouse. *The Journal of Physiology*, *311*, 307–324.

Ogawa, M. (2004). Pharmacological treatments of cerebellar ataxia. *Cerebellum (London, England)*, *3*(2), 107–111.

Perissinotti, P. P., & Uchitel, O. D. (2010). Adenosine drives recycled vesicles to a slow-release pool at the mouse neuromuscular junction. *The European Journal of Neuroscience*, *32*(6), 985–996.

Polo-Parada, L., Bose, C. M., & Landmesser, L. T. (2001). Alterations in transmission, vesicle dynamics, and transmitter release machinery at NCAM-deficient neuromuscular junctions. *Neuron*, *32*(5), 815–828.

Polo-Parada, L., Bose, C. M., Plattner, F., & Landmesser, L. T. (2004). Distinct roles of different neural cell adhesion molecule (NCAM) isoforms in synaptic maturation revealed by analysis of NCAM 180 kDa isoform-deficient mice. *Journal of Neuroscience*, *2524*(8), 1852–1864.

Polo-Parada, L., Plattner, F., Bose, C., & Landmesser, L. T. (2005). NCAM 180 acting via a conserved C-terminal domain and MLCK is essential for effective transmission with repetitive stimulation. *Neuron*, *46*(6), 917–931.

Pyle, J. L., Kavalali, E. T., Piedras-Rentería, E. S., & Tsien, R. (2000). Rapid reuse of readily releasable pool vesicles at hippocampal synapses. *Neuron*, *28*(1), 221–231.

Renden, R., & von Gersdorff, H. (2007). Synaptic vesicle endocytosis at a CNS nerve terminal: Faster kinetics at physiological temperatures and increased endocytotic capacity during maturation. *Journal of Neurophysiology*, *98*(6), 3349–3359.

Ruiz, R., Cano, R., Casañas, J. J., Gaffield, M. A., Betz, W. J., & Tabares, L. (2011). Active zones and the readily releasable pool of synaptic vesicles at the neuromuscular junction of the mouse. *Journal of Neuroscience*, *31*(6), 2000–2008.

Ruusuvuori, E., & Kaila, K. (2014). Carbonic anhydrases and brain pH in the control of neuronal excitability. *Subcellular Biochemistry*, *75*, 271–290.

Sandvig, K., Olsnes, S., Petersen, O. W., & van Deurs, B. (1987). Acidification of the cytosol inhibits endocytosis from coated pits. *The Journal of Cell Biology*, *105*, 679–689.

Shaeki, Y., & De Camilli, P. (2012). Synaptic vesicle endocytosis. *Cold Spring Harbor Perspectives in Biology*, *4*(9), a005645.

Srinivasan, G., Kim, J. H., & von Gersdorff, H. (2008). The pool of fast releasing vesicles is augmented by myosin light chain kinase inhibition at the calyx of Held synapse. *Journal of Neurophysiology*, *99*(4), 1810–1824.

Stevens, C. F., & Williams, J. H. (2000). Kiss and run" exocytosis at hippocampal synapses. *Proceedings of the National Academy of Sciences of the United States of America*, *97*(23), 12828–12833.

Tabares, L., Ruiz, R., Linares-Clemente, P., Gaffield, M. A., Alvarez de Toledo, G., Fernandez-Chacon, R., & Betz, W. J. (2007). Monitoring synaptic function at the neuromuscular junction of a mouse expressing synaptopHluorin. *Journal of Neuroscience*, *27*, 5422–5430.

Wang, L. H., Südhof, T. C., & Anderson, R. G. (1995). The appendage domain of alpha-adaptin is a high affinity binding site for dynamin. *The Journal of Biological Chemistry*, *270*, 10079–10083.

Yue, H. Y., & Xu, J. (2014). Myosin light chain kinase accelerates vesicle endocytosis at the calyx of Held synapse. *The Journal of Neuroscience : The Official Journal of the Society for Neuroscience*, *34*(1), 295–304.

Zhang, J., An, Y., Gao, J., Han, J., Pan, X., Pan, Y., … Li, X. (2012). Aquaporin-1 translocation and degradation mediates the water transportation mechanism of acetazolamide. *Plos One*, *7*(9), e45976.

Zhang, Q., Li, Y., & Tsien, R. W. (2009). The dynamic control of kiss-and-run and vesicular reuse probed with single nanoparticles. *Science (New York, N. Y.)*, *323*(5920), 1448–1453.

Zhang, Z., Nguyen, K. T., Barrett, E. F., & David, G. (2010). Vesicular ATPase inserted into the plasma membrane of motor terminals by exocytosis alkalinizes cytosolic pH and facilitates endocytosis. *Neuron*, *68*(6), 1097–1108.